Mechanical Systems and Signal Processing 112 (2018) 77–97

Contents lists available at ScienceDirect

Mechanical Systems and Signal Processing

journal homepage: www.elsevier.com/locate/ymssp

Occupant localization using footstep-induced structural vibration

Mostafa Mirshekari [a,*], Shijia Pan [b], Jonathon Fagert [a], Eve M. Schooler [c], Pei Zhang [b], Hae Young Noh [a]

[a] Civil and Environmental Engineering, Carnegie Mellon University, Pittsburgh, PA 15213, USA
[b] Electrical and Computer Engineering, Carnegie Mellon University, Moffett Field, CA 94035, USA
[c] Intel, Internet of Things Group, 2200 Mission College Blvd, Santa Clara, CA 95054, USA

ARTICLE INFO

Article history:
Received 2 December 2017
Received in revised form 1 March 2018
Accepted 15 April 2018
Available online 22 April 2018

Keywords:
Indoor occupant localization
Footstep-induced floor vibration
Adaptive multilateration
Wavelet decomposition
Dispersion
Structural vibration

ABSTRACT

In this paper, we present an occupant localization approach through sensing footstep-induced floor vibrations. Occupant location information is an important part of many smart building applications, such as energy and space management in a personal home or patient tracking in a hospital room. Adoption of current occupant location sensing approaches in smart buildings (e.g., camera, radio frequency (RF), mobile devices, etc.) is often limited due to the maintenance, installment, and calibration requirements of these sensing systems. To overcome these limitations, we introduce a new approach to use footstep-induced structural vibration for step-level occupant localization. The intuition behind this approach is that footsteps induce floor vibrations which are received in different vibration sensor locations at different times. This paper focuses on localizing a single occupant within each sensing range. To localize the footsteps, we utilize the time differences of arrival (TDoA) of the footstep-induced vibrations. However, this approach involves two main challenges: (1) the vibration wave propagation in the floor is of dispersive nature (i.e., different frequency components travel at different velocities) and (2) due to floor heterogeneity, these wave propagation velocities vary in different structures as well as in different locations in a structure. These issues lead to large localization inaccuracies or calibration requirements. To address dispersion challenge, we present a decomposition-based dispersion mitigation technique which extracts specific components (which have similar propagation characteristics) for localization. To address velocity variations, we introduce an adaptive multilateration approach that employs heuristics to constrain the search space and robustly locate the footsteps when the propagation velocity is unknown. Constraining the search space overcomes the additional complexity which is resulted from adding an unknown variable (propagation velocity). We evaluated our approach using the field experiments in 3 different types of buildings (both commercial and residential) with human participants. The results show an average localization error of 0.34 m, which corresponds to a 6X reduction in error compared to a baseline method. Furthermore, our approach resulted in standard deviation of as low as 0.18 m, which corresponds to a 8.7X improvement in precision compared to the baseline approach.

* Corresponding author.
E-mail addresses: mmirshekari@cmu.edu (M. Mirshekari), shijiapan@cmu.edu (S. Pan), jfagert@cmu.edu (J. Fagert), eve.m.schooler@intel.com (E.M. Schooler), peizhang@cmu.edu (P. Zhang), noh@cmu.edu (H.Y. Noh).

https://doi.org/10.1016/j.ymssp.2018.04.026
0888-3270/

1. Introduction

Indoor occupant localization is important for many smart building applications including energy management [1,2], space utilization and management [3–5], and healthcare [6,7]. For example, knowing the location of occupants inside a building can improve building energy management system to optimize energy efficiency while considering occupant comfort. Furthermore, it improves utilization and design of spaces such as shopping malls and offices by enabling occupant tracking which can be used for understanding occupant behaviour. Prior work has developed various sensing approaches for indoor human localization, such as vision [8,9], pressure [10,11], and Radio-Frequency (RF) [12–14]. These sensing approaches can potentially achieve high localization accuracy; however, installation, maintenance, and calibration requirements of these approaches often limit their application. Vision-based sensing needs an unobstructed line of sight between the camera and the occupants which might not be possible in indoor settings due to obstructions such as furniture and columns [9]. Pressure and non-wearable RF-based sensing need dense deployment or extensive calibration for fine-grained and step-level (0.5 m) occupant localization [11,15]. More recently, mobile-device based approaches (including wearables) have been developed, but they require the occupants to carry or wear a device, which may not be applicable in certain applications [16–20].

To overcome these limitations, vibration-based sensing is introduced for occupant localization [21–24]. This approach does not need the occupants to carry a device (i.e., is non-intrusive) and allows sparse sensor deployment compared to other sensing approaches such as pressure-based sensing (e.g., smart carpets) which need a sensor for every footstep location and RF-based sensing approaches which require either extensive training for fingerprinting or need every person to carry a device to provide a good resolution [25] However, current localization approaches for vibration-based sensing either perform only coarse-grained localization [21] or are based on detailed prior information which limits their use to only specific locations and buildings where the localization models are calibrated [22,23,26]. Calibrating these models for different locations and buildings is costly and results in deployment difficulty.

In this paper, we introduce a robust step-level occupant localization approach for heterogeneous floors that uses the footstep-induced floor vibrations. The intuition behind our approach is that when people walk, their footsteps induce structural vibrations. These vibrations travel through the floor and are received by the vibration sensors installed at various locations on the floor and at different times. These time differences of arrival (TDoA) information can then be used, together with the wave propagation velocity, for localizing the occupants through multilateration. However, the footstep-induced vibration signals are distorted as they travel through the dispersive and heterogeneous floor structure, which makes footstep localization in real floors a challenging task.

Specifically, the key research challenges are: (1) signal distortion due to dispersive floor characteristics (i.e., different propagation velocities for each frequency components) results in drastically dissimilar signal shapes for the same footstep signals measured from multiple sensors. Thus, the comparison of those signals become difficult, which leads to inaccurate TDoA estimation; and (2) wave propagation velocities are important parameters in multilateration for estimating the footstep location, but they are unknown and differ greatly across different locations of the floor and also across different buildings due to structural heterogeneity. Unknown propagation velocity either requires extensive calibration, which is time-consuming and costly, or adds to the dimension (i.e., number of unknowns) of the multilateration (which is a highly non-convex problem) and results in large localization errors.

To address these challenges, we introduce a combination of decomposition-based dispersion mitigation technique (for the first challenge) and adaptive multilateration approach (for the second challenge). The dispersion mitigation technique decomposes the signal into different frequency components, obtains TDoA for each component separately, and then combines the results from the components with low localization error. By separating signals into different components each of which has similar wave propagation characteristics, we reduce the dispersion-induced signal distortions and thus improve the TDoA estimation accuracy. Then, the adaptive multilateration approach employs heuristics about the space configuration to define a novel formulation to be minimized across a constrained search space (i.e., footstep location and propagation velocity). By constraining the search space, we reduce the effect of non-convexity (which might result in erroneous local minima) to robustly estimate location when the propagation velocity is unknown and changes for different locations. As a result, our approach enables step-level footstep localization in heterogeneous structures without requiring extensive calibration. We validate our approach through field deployments in 3 types of structures with indoor pedestrians.

In summary, the core contributions of this paper are:

- We introduce a robust fine-grained step-level occupant localization approach using footstep-induced floor vibration (in Section 4.1).
- We characterize dispersive wave propagation properties of floors. We exploit these properties to mitigate signal distortions, by decomposing the signals before TDoA estimation (in Section 4.3).
- We make our approach adaptive to structural heterogeneity by modeling heuristics on space configurations that constrain the search space. This enables robust footstep location estimation without an extensive wave propagation velocity calibration requirement (in Section 4.4).

The remainder of the paper is structured as follows: in Section 2 we review the literature for source localization algorithms and their limitations. In Section 3 we discuss the physics behind our approach, and in Section 4 we describe the detailed method of localizing occupants using footstep-induced floor vibrations. Next, in Section 5 we describe the experiments we conducted in several structures and then discusses the results and the performance of our system. Finally, we present future work and conclusions in Sections 6 and 7, respectively.

2. Related work

The occupant localization using footstep-induced floor vibrations can be seen as a source localization problem in dispersive media. Here, we explore the existing approaches and remaining research gap for vibration-based occupant localization.

2.1. Dispersion-induced signal distortion reduction

Floor structures are dispersive which causes waves of different frequency to travel at different speed. This results in signal distortions which decrease the accuracy of TDoA estimation and localization (see Section 3 for details). The two main approaches to mitigate such distortions are physics-based approaches [27–30] and signal-based approaches [31–36]. The physics-based approaches require a priori information (e.g., stiffness and mass) of the underlying structure to estimate dispersion curves. However, their application is limited in real environments as this information varies for different structures and requires extensive calibration. Signal-based approaches address dispersion by decomposing the signals using time–frequency representations (TFR) and do not require detailed prior information about the floor.

Among the TFR approaches, wavelet decomposition has been successfully utilized for impulsive excitations (such as footstep-induced vibration) because it is suitable for representing non-stationary signals [35,24,26,32–34,37]. The main wavelet-based approaches for source localization either utilize: (1) the ridge [32,33,37,35] (i.e., peak amplitude in scale-time plane) which is difficult to robustly estimate in real floors with environmental noise or (2) highest energy scale components [26,24] which potentially have large noise (ambient vibration) because this scale might correspond to the fundamental frequency of the floor. Therefore, these approaches are not well-suited for source localization and result in large errors. To improve localization, We introduce a new approach which directly chooses the components with the highest localization performance for signal recovery (localization performance will be described in Section 4.4).

2.2. Source localization

Source localization problems consider signals induced by a source of unknown location and received in several sensors at known locations to find the source location. Source localization is of vital importance in several domains such as sonar [38,39], mobile communications [40,41], wireless sensor networks [42,43], structural health monitoring [44–46], and robotics [47,48]. Existing approaches include beamforming, fingerprinting, and multilateration.

Beamforming delays/shifts the received signals based on an assumed waveform and propagation velocity and then finds the location by identifying the time-shift that maximizes the similarity in the delayed signals [49,46,50,51]. These approaches in general focus on propagation in homogeneous media where the propagation velocity is well known (e.g., sound in air). In these approaches, unknown propagation velocity and dispersion-related signal distortions would result in large localization errors.

Fingerprinting (or signature-based) approaches are an alternative when the propagation characteristics are unknown. These approaches first construct a database of received signals for source excitation in different known locations through site surveying. For every new excitation, the measured signals will be compared to the signals in the database to find the location corresponding to the most similar signal [52–54]. Unfortunately, the site surveying can be a time-consuming and laborious process, especially for fine-grained localization.

Range-based localization estimates the range between the source and sensors and leverage such information for estimating source location. Two methods introduced for range estimation are Received Signal Strength (RSS)-based and Multilateration. RSS-based [55–57] methods estimate the range between the source and the sensors based an attenuation pattern for wave propagation. However, these methods do not perform well in real floors for which such attenuation pattern is not previously known or accurately modeled by a parametric model (such as exponential models as assumed in [57]). This becomes more problematic especially when reflections can create constructive or destructive interference. Multilateration, on the other hand, leverages the differences in time of arrival for signals received by different sensors, referred to as TDoA, to estimate the location of the source [58–65,37]. For a specific value of TDoA between two sensors, the possible solutions (i.e., source locations) form a hyperbola. The location of the source can be estimated by adding more sensors and their TDoAs, which result in more hyperbolas, and then finding their intersection. In this regard, a cost function for each potential source location is defined as the error between (1) the distance difference between the potential source location and the known sensor locations and (2) their expected distance difference computed from the TDoA and wave propagation velocity. The solution of multilateration is obtained by minimizing this function. In this paper, we adopted the multilateration approach as it locates the source in a fine-grained manner without laborious site surveying and does not assume a known waveform.

A key challenge in multilateration is that if the wave propagation velocity is unknown and varies across different locations and buildings, which is often the case in practice, it increases the number of unknowns and the non-convexity of the multilateration cost function. The severe non-convexity of the cost function makes finding the global minimum difficult. Therefore, we introduce an adaptive multilateration approach that is more robust to irrelevant local minima by incorporating space configuration information to heuristically limit the search space.

3. The physics behind footstep-induced structural vibrations

Our localization approach utilizes wave propagation in floor structures. In this section, we provide a brief background of the physics behind footstep-induced structural vibration and describe the main challenges we address: (1) dispersion-related signal distortions and (2) unknown wave propagation velocity across different locations due to floor heterogeneity.

The impact due to each footstep strike is of an impulsive nature. These impulses result in deformation (and restoration due to elasticity) in the floor. This combined deformation and restoration results in waves propagating outward from the footstep location through the floor. These waves are plate waves (i.e., lamb waves) because building floors are generally solid plates with free boundaries on top and bottom and the ratio of wavelength to thickness of the floor is large in our application [66]. As an example, if the wave have a frequency component of 100 Hz and wave propagation at a velocity of 300 m/s, the wavelength is equal to 3 m, which is much larger than the common floor thickness (on the order of 0.2–0.3 m).

However, lamb wave propagation in floor structure is of a dispersive nature, which causes different frequency components to have different phase velocities [67,68]. Due to this dispersion effect, the same footstep will induce dissimilar signals in sensors in different parts of the floor. In other words, dispersion introduces distortion in the vibration signal, which makes vibration-based occupant localization a challenging task. Fig. 1 shows a simple and intuitive illustration of dispersion to better understand how it distorts the signals. In this figure, we assume that the wave consists of two linearly attenuative sinusoidal components of 2 and 8 Hz. Fig. 1a and b show the waves propagated through a non-dispersive medium in which wave propagation velocity is the same for all frequency components. Fig. 1c and d show the waves propagated through a dispersive medium in which wave propagation velocities are different for different frequency components. Fig. 1a and c show the wave measured at a closer sensor and Fig. 1b and d show the resulting wave measured at a further sensor. As shown in these figures, in a non-dispersive medium, the waves arrive at a later time (with delay of Δ) in the further sensor, but the shape of the signal is the same as the one measured at the closer sensor. In contrast, in the dispersive medium, the further sensor observes the more dispersed waves, and for the same excitation, the shape of the received signals are different for the two sensors. The difference is caused by the different delays for these two components (Δ_1, Δ_2). For example, the maximum cross-correlation values between the two sensor measurements decrease from 1 to 0.69 when the floor becomes dispersive.

In real life applications, these effects are aggravated due to reasons such as having more frequency components, different attenuation rates, and noise [26]. These dispersion-related distortions make it difficult to estimate the TDoA between different sensors, thereby decreasing the localization accuracy.

Furthermore, lamb wave propagation velocity (for each frequency component) depends on structural and material characteristics, such as modulus of elasticity, density, Poisson's ratio, and slab thickness [69]. Due to structural heterogeneity, these characteristics (and thus the propagation velocity) vary greatly across different sections of the floor and different buildings. To handle this velocity variations, we assume that heterogeneous floors are locally isotropic. In other words, the structural characteristics and wave propagation velocity differ across different footstep locations; however, in the vicinity of each footstep location, these characteristics (and propagation velocity to the sensors) are assumed to be similar. Then

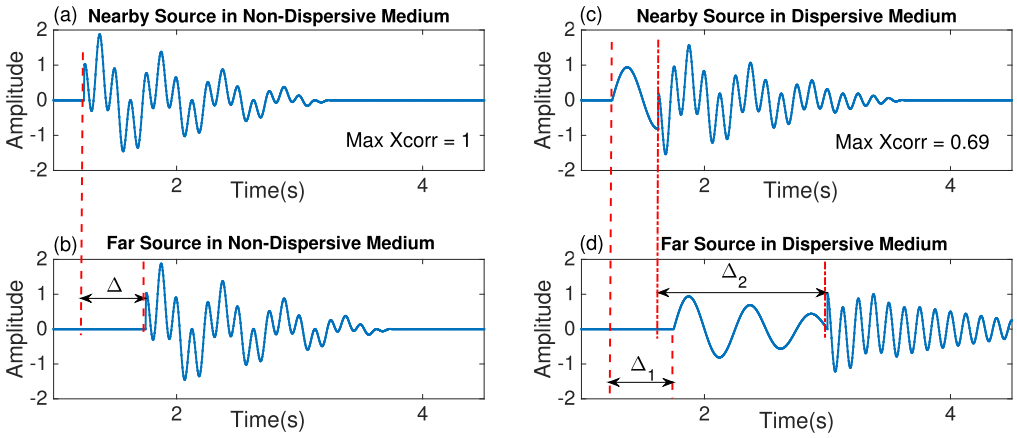

Fig. 1. Dispersion illustration: This figure illustrates how dispersion distorts the shape of the received signals by considering two attenuative sinusoidal components. These distortions decrease the localization accuracy. The red lines show the arrival time of sinusoidal components. (For interpretation of the references to colour in this figure legend, the reader is referred to the web version of this article.)

to eliminate extensive calibration to obtain wave propagation velocity in different footstep locations, we introduce our adaptive multilateration approach in the next section.

4. Occupant localization approach

In this section, we describe our vibration-based localization approach. We start by presenting an overview of the different modules of the approach (Section 4.1) followed by a detailed description of how the system distinguishes footsteps from other impulsive excitations (Section 4.2) accounts for dispersion (Section 4.3), and adapts to heterogeneous floors (Section 4.4).

4.1. Approach overview

Our fine-grained floor vibration-based occupant localization approach has three main modules, as shown in Fig. 2: (1) Footstep Detection; (2) Dispersion-invariant TDoA Estimation; and (3) Locally Adaptive Footstep Localization. In the Footstep Detection module, our method first senses the ambient floor vibrations with multiple sensors. Then, it classifies the vibration events to extract the footstep-induced signals. The details of this module is discussed in Section 4.2. Next, in the Dispersion-invariant TDoA Estimation module, our approach mitigates the dispersion-induced signal distortion through signal decomposition and then estimates the TDoAs for different components. Section 4.3 provides more details on the dispersion mitigation approach. Finally, in the Locally Adaptive Footstep Localization module our method selects a subset of sensors which are closest to the footstep to further reduce signal distortion effects and estimates component-level footstep location using our adaptive multilateration approach. Then, it selects a subset of components with best multilateration performance and averages these component-level location estimations to obtain the final estimation of the footstep location. The details of this module are discussed further in Section 4.4.

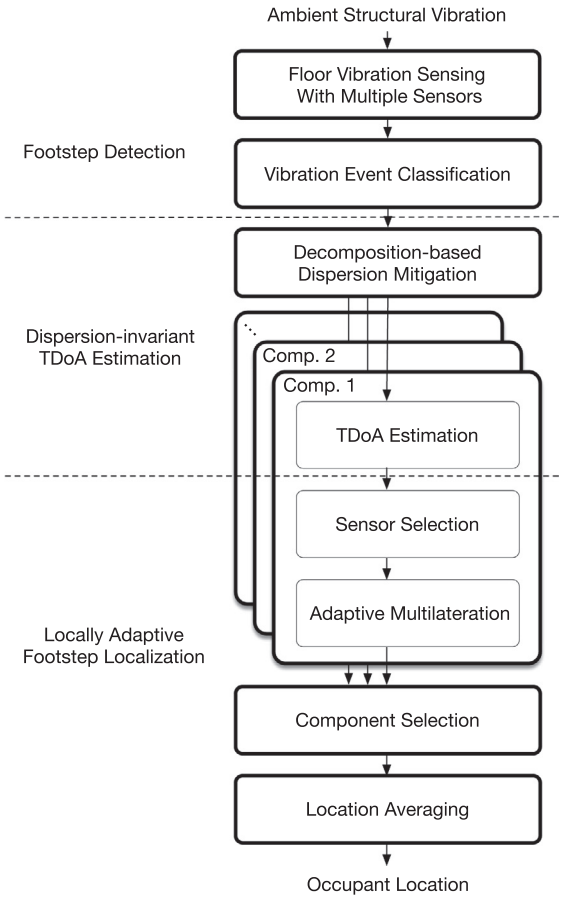

Fig. 2. Occupant localization approach overview.

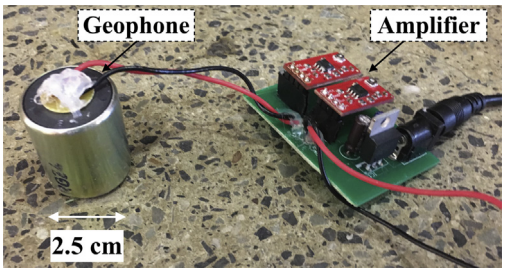

Fig. 3. The sensing unit. The geophone measures the velocity of vertical vibration on the floor which then will be amplified, digitized, and transferred to PC for further analysis.

4.2. Footstep detection

The footstep detection module first measures the vertical floor vibrations using geophone sensors placed on the floor at different locations. Geophones are low-cost and low-distortion sensors which convert the velocity of the floor vibration to voltage. The vibration signals are then amplified using an op-amp to improve their resolution [70]. Then, the vibration signals are digitized and transferred to PC for further analysis. An example of the sensing system is presented in Fig. 3.

Generally, the collected vibration signals are mixtures of footsteps, other impulsive excitation (such as falling objects and door shutting), and background noise (such as fan, machinery, and sensor noise). To extract footstep-induced signals, we (1) use an anomaly detection algorithm to separate impulsive vibration events from the background noise (an example is presented in Fig. 4) and and then (2) classify the extracted vibration events into footsteps and non-footsteps using a one-class SVM classifier [71,72]. Distinguishing footsteps prevents the system from localizing irrelevant impulsive excitations.

To extract the impulsive vibration events, we conduct a chi-squared hypothesis test. The main intuition is that the variance of the impulsive event signal is larger than the variance of the ambient noise signal. To this end, we use the Chi-squared test that determines whether the signal has the same variance as the ambient noise. In other words, the Chi-squared test evaluates the null hypothesis $H_0 : \sigma_w^2 = \sigma_n^2$ (i.e., signal is a noise) against the alternative hypothesis $H_1 : \sigma_w^2 > \sigma_n^2$ (i.e., signal is an impulsive event), where σ_w^2 is the variance of the signal window and σ_n^2 is the variance of the ambient noise. We use the sliding window on the signal and conduct the hypothesis test for each window to detect impulsive vibration events. We have empirically chosen one tenth of a second as the window size to ensure that the beginning part of the footstep vibration signal is detected. The reason behind choosing the Chi-squared test is that the variance of the ambient noise signal follows a scaled Chi-squared distribution. Specifically, assuming normally distributed and independent noise measurements, the following statistics (i.e., χ^2-statistics) for each window has a Chi-squared distribution [73]

$$\chi_w^2 = (m-1)\frac{s_w^2}{\sigma_n^2}, \tag{1}$$

where m is the number of samples in the signal window, and s_w is the sample variance of the signal within the window.

We continuously and incrementally [74] learn and update the population variance of the ambient noise, σ_n^2, from the sensed data using the following equations.

$$\mu_n[h] = \mu_n[h-1] + \frac{1}{h}(x_n[h] - \mu_n[h]) \tag{2}$$

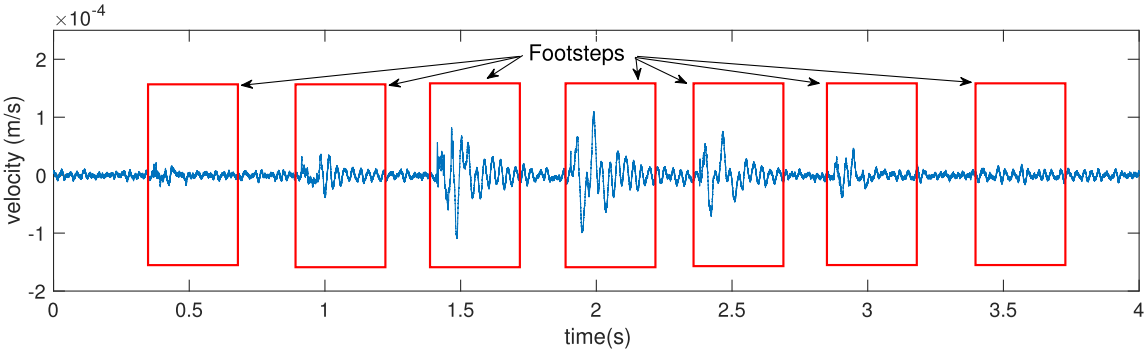

Fig. 4. An example of footstep-induced floor vibration signals measured by a geophone.

$$\sigma_n^2[h] = \frac{(h-1)\sigma_n^2[h-1] + (x_n[h] - \mu_n[h-1])(x_n[h] - \mu_n[h])}{h}, \tag{3}$$

where $x_n[h]$ is the h^{th} measurement for ambient noise signal, $\mu_n[h]$ and $\sigma_n^2[h]$ are the updated mean and variance of the ambient noise signal after adding the h^{th} measurement.

When the signal form deviates from the ambient noise, the corresponding statics, χ_w^2, also deviates from the chi-square distribution. Thus, for every signal window, we compare the χ_w^2-statistics with χ_α^2, which is the statistic value corresponding to the significance levels of α (i.e., the probability of having samples with χ^2-statistics higher than χ_α^2 given the null hypothesis). Specifically, we reject the H_0 if $\chi_w^2 \geqslant \chi_\alpha^2$ [73]. The significance level is the false positive rate of the test (i.e., the probability of rejecting the null hypothesis when the it is true). In this work, we empirically choose significance value of 0.01. The windows in which the null hypothesis is rejected correspond to the vibration events and are used for classifying the footstep-induced vibrations based on the one-class SVM [71,72].

4.3. Dispersion-invariant TDoA estimation

To mitigate dispersion-related signal distortion, we decompose the vibration signal using a time frequency representation (TFR) and extract scale components from each sensor data [26]. Separately analyzing each component, which has similar wave propagation characteristics (e.g., phase velocities), mitigates the effects of dispersion as shown in Fig. 5. This figure shows the signals received in two sensors from the same footstep excitation. After decomposition (and extracting a specific component), the shapes of the signals become more similar to each other (the maximum cross-correlation value increases from 0.49 to 0.95, which corresponds to 1.9X improvement in similarity) and show more clear peak correspondence.

4.3.1. Decomposition-based dispersion mitigation

To decompose the signal, we use wavelet transform, which is well suited for non-stationary signals such as impulses and footsteps [33,34,75] (as discussed in Section 2.1). We decompose the signal into frequency components using continuous wavelet transform. Mathematically, continuous wavelet decomposition of signal x can be represented as,

$$T(a,b) = w(a) \int_{-\infty}^{+\infty} x(s) \Psi_{b,a}^*(s) ds \tag{4}$$

in which $w(a)$ is a weighting function and $\Psi_{b,a}(s)$ is the dilated and time-shifted version of the basis function (mother wavelet $\Psi(s)$), which can be represented as,

$$\Psi_{b,a}(s) = \Psi\left(\frac{s-b}{a}\right) \tag{5}$$

in which b is the unit of translation in time and a is the amount of dilation (commonly called a scale). This dilation (i.e., scale) is inversely proportional to the frequency components of the signal. In other words, higher scales correspond to lower frequency components and the relationship between them can be described using [75],

$$F_a = \frac{F_c}{a\delta} \tag{6}$$

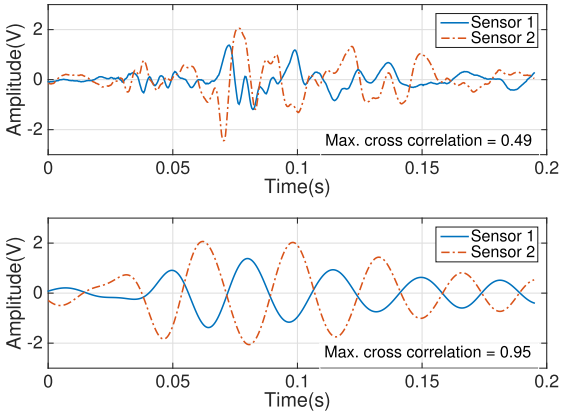

Fig. 5. An example of dispersion mitigation by signal decomposition. This figure shows that the decomposed signals (bottom) are more similar, and the peaks clearly correspond with each other the improvement compared to the raw signals (top) received in two sensors for the same excitation.

in which δ is the sampling frequency (Hz), F_a is the (pseudo-) frequency (Hz) corresponding to scale of a, and F_c is the center frequency of the wavelet (Hz).

Mexican hat wavelet is chosen as the mother wavelet as it is a good representation of the footstep-induced vibration signals due to its similarity in shape [76]. To reduce the computational cost of performing the continuous wavelet transform, we choose a limited range of scales. To limit the range (while keeping the useful information in the signal), we use two notions: (1) floor vibration signals caused by footsteps typically contain frequencies below 100 Hz [77] and (2) geophones are naturally a second-order high pass filter for frequencies less than 10 Hz [78,79] (i.e., when the frequency decreases from 10 Hz to 1 Hz, the geophone's response may become 100 times weaker). Therefore, we choose the range of 10–100 Hz for wavelet decomposition. Using Mexican hat wavelet, for sampling frequency of 25 kHz, which we used for evaluation in Section 5.1, this range translates to a scale range of 64–640. We have observed in our prior experiments that footwear can affect the frequency range. For example, high heels are more similar to impulses (e.g., ball drops) than flat-bottom shoes and hence, generally result in higher frequency components compared to, for example, someone wearing flat-bottom shoes [25]. However, while we did not control the footwear of the subjects, there was little variation in the footwear of the experimental subjects (all variants of flat-bottom shoes). The defined range works well for the structures and footwear we consider in Section 5. This range can be modified to accommodate different applications with different floor types or footwear with different response frequencies.

4.3.2. TDoA estimation

To estimate the TDoAs between different pairs of sensors for every scale components, we utilize a threshold-based method [80]. This method detects the first peaks of the signals, which correspond to the wave arrival time at each sensor location. Note that the wave arrival time does not provide the time of flight because the start time (i.e., time of footstep excitation) is unknown. Instead, the TDoA is obtained by comparing the wave arrival times of each sensor pairs. We have chosen the peak detection method over the cross-correlation to compute the TDoA because it is less affected by signal distortions due to multipath and reflections [81]. The peaks are determined using the anomaly detection approach, which assumes that the signal has a Gaussian distribution for the background noise (i.e., when there is no footstep). This assumption is then used to find the threshold for detecting an anomaly (i.e., time of arrival for a footstep event). We chose 3σ as a threshold, in which σ is the standard deviation of the decomposed background noise, to allow 1% detection false alarm. This threshold value is adjustable according to the application.

4.4. Locally adaptive footstep localization

To enable footstep localization in different structures and heterogeneous floors, we present a locally adaptive multilateration approach which robustly estimates the footstep location when the propagation velocity is unknown. We take a two-step approach to first obtain the component-level location estimation through sensor selection and adaptive multilateration and then combine those results to make the system-level location estimation.

4.4.1. Sensor selection

The key intuition behind choosing the closest sensors is that the less distance waves propagate through the floor, the less it gets affected by the floor's attenuative characteristics. This in turn results in higher SNR, less signal distortion, and consequently more accurate TDoA and location estimation. To choose the closest sensors, we utilize the relative time of arrival for footstep signals to reach different sensors. We first sort the detected times of arrival for first peaks for different sensors obtained in the previous module and then select the sensors with earlier times of arrival. Note that each scale component may lead to different set of "closest sensors" due to the errors in the first peak detection; however, the components with such erroneous peak estimations often lead to large localization errors and get filtered out through the component selection in the next module. Assuming unknown wave propagation velocity, at least four sensors are necessary for localizing the footsteps. Using more sensors has the potential to reduce the noise and improve the accuracy; however, including additional sensors means including the sensors further away from the footstep (because of our sensor selection approach), which result in more attenuated signals and lower localization accuracy. Thus, in this paper, we use four sensors, whose performance is compared with systems with different number of sensors in Section 5.2.3.

4.4.2. Adaptive multilateration

These selected sensors and their corresponding TDoAs are then utilized in our adaptive multilateration approach to estimate the location of the footstep for each scale component (component-level location estimation). Our approach does not require prior knowledge on wave propagation velocity; therefore, it can adapt to different locations in a heterogeneous floor (with different structural characteristics).

The main challenge in achieving the adaptive localization is the large search space for solutions, due to the model flexibility (e.g., extra unknown parameters on wave propagation velocity). As discussed in Section 3, we assume different propagation velocities across different locations (i.e., heterogeneous floor) and same velocity between each footstep and the sensors (i.e., locally isotropic). However, due to the non-convexity of the problem, deviation from local isotropy assumption causes the multilateration to get stuck in local minimas and therefore result in large localization errors.

To make the multilateration approach more robust, we employ heuristics on physical space configurations to constrain the solution search space (i.e., possible locations and velocities). We constrain the search space by considering the propagation velocities for which every pair of hyperbolas have an intersection in the room boundary. As discussed in Section 2.2, the possible locations of a footstep for specific TDoA between two sensors and propagation velocity form a hyperbola. Ideally, these hyperbolas from multiple sensor pairs meet at one intersection, which is the solution of multilateration; however, signal noise and errors in TDoA estimation lead to hyperbolas that meet at multiple points or do not intersect. To this end, we define the localization cost function as: (1) the area of the polygon between intersections of hyperbolas when all pairs of hyperbolas intersect in the room boundary or (2) an arbitrarily large value when they do not intersect (e.g., ∞). This cost function is then minimized across different propagation velocities to robustly estimate the location of footsteps.

The advantages of our approach are that: (1) it does not require wave propagation velocity to be known and fixed and (2) constraining search space makes it less-prone to vastly out of range local minima. Fig. 6a–c visualize an example of the multilateration procedure. These figures show the hyperbolas for three different velocities (100, 150, and 200 m/s), where the true velocity is 200 m/s. For each velocity, we construct the hyperbolas and find their intersections. We can see from the figures that by minimizing the area, its center point (found by averaging the intersection locations) gets closer to the actual location of the footstep (represented by a star sign). In other words, the case with minimum area between intersections also has the lowest localization error.

Our approach uses a closed-form formulation for constructing the hyperbolas, finding their intersections, and forming the polygon between the intersections. In the closed-form formulation, for a specific value of wave propagation velocity, the hyperbola between a pair of sensors is defined in the following format [82].

$$x = \frac{p_{ix} + p_{jx}}{2} + X\cos\alpha - Y\sin\alpha \tag{7}$$

$$y = \frac{p_{iy} + p_{jy}}{2} + X\sin\alpha + Y\cos\alpha \tag{8}$$

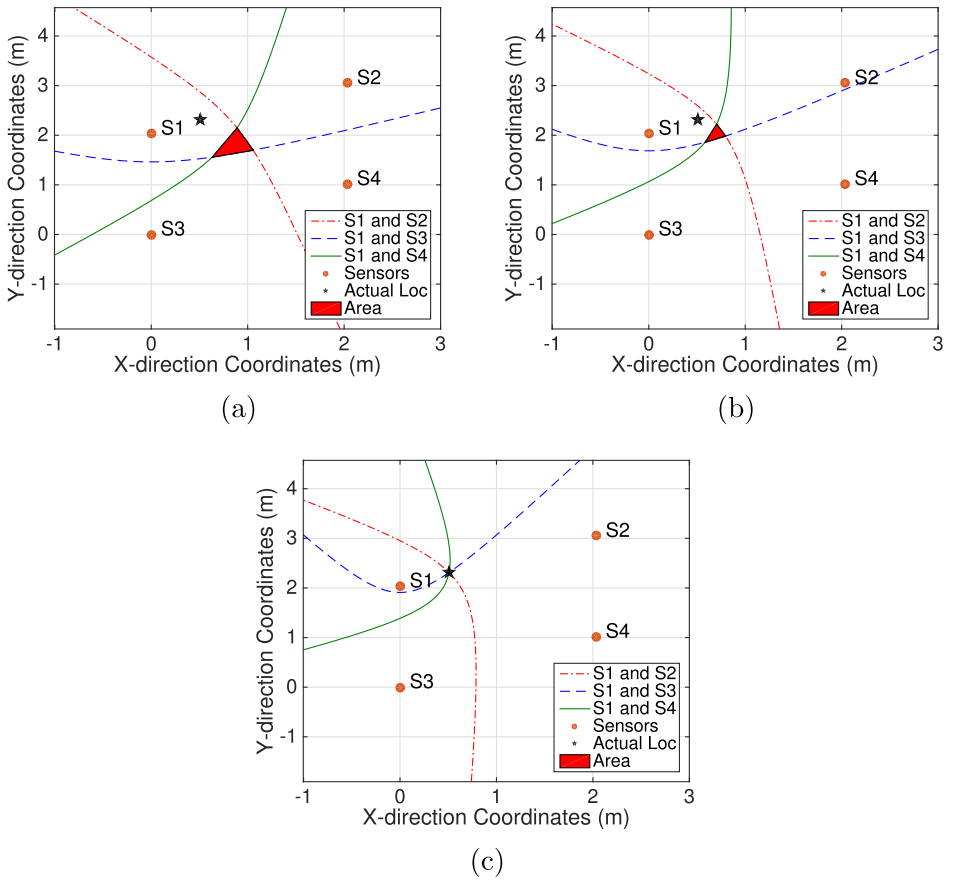

Fig. 6. An example of the solution procedure. The footstep location can be found by changing the velocity values and finding the velocity value which minimizes the area between intersections. Parts a–c show an example of such a procedure for three values of wave propagation velocity. We can see that the case with minimum area between intersections also has the lowest localization error.

where α is the rotation angle of the hyperbola, $[x, y]$ are the coordinates of the hyperbola, and p_{ix}, p_{iy}, p_{jx}, and p_{jy} are the coordinates of the sensors i and j. Also,

$$cos\alpha = \frac{p_{ix} - p_{jx}}{2c}; \qquad sin\alpha = \frac{p_{iy} - p_{jy}}{2c}; \qquad X = a * cosh(\theta); \qquad Y = b * sinh(\theta) \tag{9}$$

in which θ is a parameter which can range $[-\infty, +\infty]$. Furthermore, a, b, and c are defined as,

$$a = \frac{v\tau_{ji}}{2}; \qquad b = \sqrt{c^2 - a^2}; \qquad c = \frac{1}{2}\left\|p_j - p_i\right\|_2 \tag{10}$$

in which v is the propagation velocity and τ_{ji} is the time difference of arrival between the i^{th} and j^{th} sensor. Using this formulation, one of the sensors is considered as the anchor sensor and a hyperbola is found between the anchor sensor and every other sensor. We then use a grid-search based method [83] to find the intersections of the hyperbolas.

The final step of our solution is to minimize the area of the resulting polygons across a range of velocity values. Let the intersections between different pairs of hyperbolas which are in the boundary of the room be stored in an array called P in which $P_k = [x_k, y_k]$. Then the optimization objective is defined as

$$min_v \left(\begin{cases} \sqrt{\frac{1}{2}\sum_{k,l=1}^{3} \|P_l - P_k\|_2^2} & if \ |P| = \frac{n(n-1)}{2} \\ \infty & if \ |P| \neq \frac{n(n-1)}{2} \end{cases} \right) \tag{11}$$

where $\|P_l - P_k\|_2$ is the Euclidean distance between the k^{th} and l^{th} intersections, $|P|$ is the cardinality (number of elements) in the set P, and $\frac{n(n-1)}{2}$ is the number of different combinations of two hyperbolas (each representing one intersection) when there are n hyperbolas. By minimizing this cost function, we ensure that: (1) all pairs of hyperbolas intersect in the room boundary and (2) the area between these intersections is minimized. The center of the smallest area, found by averaging the intersection locations, is the component-level location estimation.

4.4.3. Component selection and location averaging

Finally, we choose a subset of component-level location estimations and use their average as the final footstep location estimation. By averaging several estimated locations, we reduce the effect of noise and outliers. The components with best localization performance are selected (i.e., components with lowest values of minimum localization cost function value as defined in Eq. (11). The lower minimum localization cost function means that the localization has been more successful (i.e., higher localization performance). In ideal scenarios and when there is no noise in the TDoAs, the minimum of this cost function is equal to zero (high localization performance). However, having noise in the TDoAs results in a larger minimum of cost function, as the hyperbolas might not intersect at one point. Therefore, we choose a subset of component-level estimated locations which result in lowest minimum localization cost function. The number of the estimated locations to be included in the subset poses a trade-off. On one hand, utilizing more scale components reduces the effect of noise and improves localization. On the other hand, including scale components with large noise decreases the localization accuracy. In this paper, we utilize eight scale components based on empirical evaluation, which is discussed further in Section 5.3.

5. Occupant localization evaluation

To understand the system performance, we conducted a set of experiments with human participants. We first introduce the sensor configuration (Section 5.1). Next, we present and analyze the footstep localization accuracy and robustness using our approach (in Section 5.2). Then, we explore the effect of decomposition-based dispersion mitigation on localization (in Section 5.3). Finally, we validate our locally adaptive localization approach using experiments in categorically different structures (in Section 5.4).

5.1. Experimental setup

To evaluate our localization approach, we utilize a sensing system which measures the footstep-induced vibration using nine floor-mounted geophones [79]. As discussed in Section 4.4.1, four sensors are necessary for localization in a real applications. However, to explore the effects of different number of sensors on localization performance, we deliberately installed a dense configuration. The collected signals are amplified by the orders of 200-2000× using an op-amp to improve the resolution of signals while reducing the amount of signal clipping. Higher signal resolution in turn improves TDoA and localization accuracy. After amplification and depending on the structure type and footstep strike energy, the effective sensing range of our system for footstep detection is up to 20 m in diameter. Amplified signals are then digitized and transferred to a server using a 24 bit A/D converter. Fig. 3 shows one of the sensing units. Sampling frequency is chosen as 25 kHz to ensure enough time resolution for accurate TDoA estimation.

The experiments include having three subjects walk in three buildings of different structural types to show that our approach is robust to different structures. All the subjects wear variants of flat-bottom footwear. The chosen structures

represent common types of structures for residential and commercial buildings and include a non-carpeted concrete hallway on the ground level of the campus building at Carnegie Mellon University (with the first observed natural frequency of 23.83 Hz), a carpeted metal deck floor on the second floor of a senior care facility (with the first observed natural frequency of 14.84 Hz), and a wooden floor in the second floor of a residential building (with the first observed natural frequency of 16.02 Hz). The tested areas did not include obstructions such as structural walls underneath or beams. Twenty walking traces, each consisting of six footsteps, are collected from each structure. The averages and standard deviations of subjects walking speed are 1.09 and 0.115 m/s for subject 1, 0.66 and 0.03 m/s for subject 2, and finally 0.84 and 0.06 m/s for subject 3. Fig. 7 presents the sensor configuration and footstep locations. Fig. 8 shows the 3 experiment locations with our system set up. The dimensions of sensor configuration represent hallways in common residential and commercial buildings. Furthermore, to obtain the ground truth, the locations of the footsteps were taped on the floor and the participants were asked to walk on these locations.

5.2. Footstep localization evaluation

In this section, we evaluate the accuracy and robustness of our localization approach which employs footstep-induced floor vibrations for occupant localization. To this end, we first discuss the accuracy of our approach for three structures. Then, we characterize the robustness of our approach for different SNR levels, footstep-sensor distances, and number of sensors.

5.2.1. Overall localization accuracy evaluation

To evaluate the accuracy of our approach, we compare the overall localization errors in all three structures using our approach and a baseline approach. The baseline approach is a method commonly used for localization which utilizes the raw signal for TDoA estimation and then performs multilateration through Nonlinear Least Square (NLS) solution. The metric used for this purpose is the Euclidean distance of the actual location of the footstep from the estimated location. Table 1 and Fig. 9 show the overall results of this comparison for all three structures' data combined. Based on these results, our approach results in 0.41 m average accuracy which is equivalent to approximately 5X improvement over the conventional approach which has 2.04 m of accuracy. Similarly, our approach results in 0.23 m standard deviation which is 6.70X precision improvement over the conventional approach. Similarly, our approach results in 3.08X and 11.38X improvement in the median and 25–75 percentile of the localization error, respectively. This level of occupant localization accuracy and robustness makes our approach more suitable for smart building applications discussed in Section 1.

5.2.2. Robustness to sensor-footstep distance

Sensor-footstep distance is an important factor in localization performance. To evaluate this factor, we use four sensors and evaluate the errors for footsteps of different locations. The metric used to define the sensor-footstep distance is the root mean square (RMS) of the the Euclidean distances of the footstep to each sensor. Furthermore, we consider two different sensor configurations to evaluate whether it is important for the footstep to be inside the polygon formed by the sensors. The first configuration consists of S4, S5, S7, and S8 and considers the three footsteps outside the polygon formed by the 4 sensors, as shown in Fig. 7. Fig. 10a depicts the changes in localization error for this configuration with respect to the defined metric. The correlation coefficient of 0.82 shows that there is a strong linear relationship between the distances and the localization error. The positive slope of 1.44 shows that higher distances result in lower localization accuracy.

The second configuration consists of S1, S2, S7, and S8. As can be seen in Fig. 7, for this configuration all the footsteps are inside the sensor polygon. Fig. 10b presents the changes in the localization error with varying sensor to footstep distances in

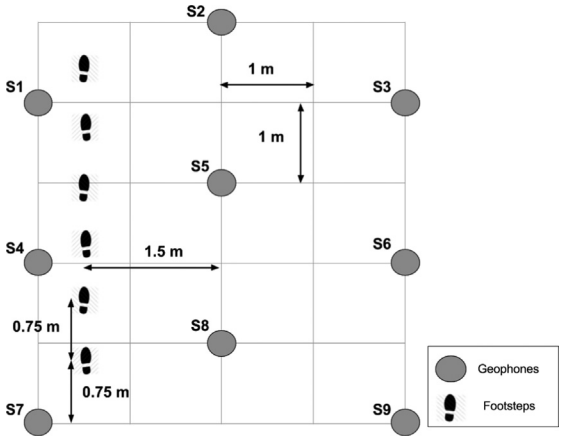

Fig. 7. Experimental setup. This figure shows the sensor configuration and the location of footstep excitations. The database includes 20 traces of six footsteps.

Fig. 8. Experiment locations. Part (a) shows a concrete non-carpeted hallway on the ground level in the campus building of Carnegie Mellon University. Part (b) is a hallway on the second floor of a senior care facility with a concrete metal deck floor. Finally, Part(c) is a room with a wooden floor on the second floor of a residential building.

Table 1
Localization results (for all three structures).

	Mean	St. Dev.	Median	Quartile
Conv. approach	2.04	1.54	1.17	2.96
Our approach	0.41	0.23	0.38	0.26
Improvement	4.98X	6.70X	3.08X	11.38X

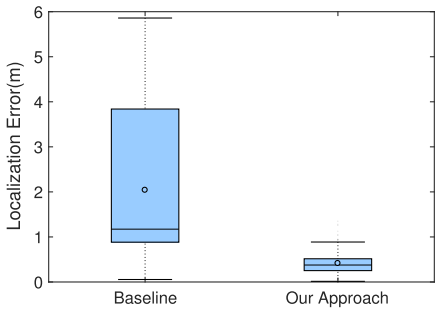

Fig. 9. Localization accuracy of our approach. This figure compares the accuracy of our localization approach with a baseline approach. Median of the results using our approach is 0.38 m which shows 3.08X improvement over the baseline approach.

this sensor configuration. In this case, compared to the results outside the polygon, both the slope (i.e., 0.16) and the correlation coefficient (i.e., 0.05) are smaller. Inside the polygon, the localization results are not as significantly affected by the distances as outside the polygon. For example, in the cases outside the polygon, increasing the distance from 2 m to 2.6 m causes the error to increase from 0.6 to 1.5 m; whereas, for a similar range of distances (2.3–2.6 m) and for the cases inside the polygon, the error increases from 0.53 m to 0.64 m. Finally, Figs. 10b and c show that as the sensors are further apart (Fig. 10b), the average localization errors are larger (0.53–0.83 m) than when we apply the sensor selection algorithm (Fig. 10c, 0.2–0.49 m). The reason is that our sensor selection algorithm chooses the closest sensors from the footstep location.

Increasing the distance the wave propagates through the floor results in more attenuation of the signal which in turn causes larger localization errors. Therefore, selecting the sensors closest to the footstep for localizing the footsteps improves the performance of localization approach and therefore is adopted in this paper (discussed in Section 4.4.1). In addition, choosing the sensor configuration (and the distance between the sensors) depends on the desirable localization accuracy (which is application-dependent). For example, in our setup and according to Figs. 10b and c, a 5 m by 2 m sensor configuration achieves 0.63 m accuracy whereas a 2.5 m by 2 m achieves 0.34 m localization accuracy. This means that, for example, six sensors are required to achieve approximately 0.63 m accuracy in a 10 m by 2 m hallway (or six sensors to cover an 8 m by 8 m room). The required number of sensors increase if the desired localization accuracy is 0.34 m.

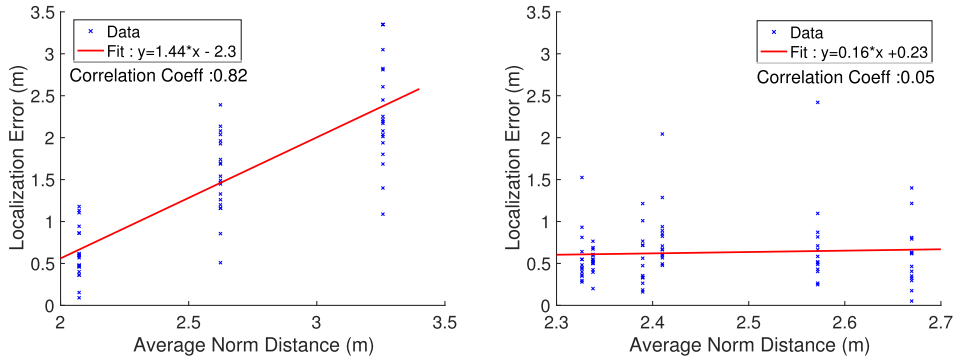

(a) S4, S5, S7, S8 (Out. sensor poly.) (b) S1, S2, S7, S8 (In. sensor poly.)

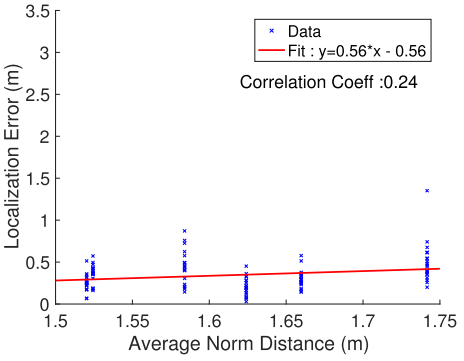

(c) Our sensor selection approach

Fig. 10. Effect of distance between footsteps and sensors on localization accuracy. This figure shows that footsteps out of the polygon (Part (a)) are generally more sensitive to distance than the footsteps inside the polygon (Part (b) and (c)). Furthermore, as the sensor selection chooses the closest sensors, Part (c) shows the smallest the localization errors.

5.2.3. Robustness to the sensor configuration

The number of sensors and the distances between them affect localization accuracy and is important for sensor selection, as described in Section 4.4.1. Generally, the trade-off is: (1) having more sensors mitigates the effect of noisy sensors and increases localization accuracy; (2) high footstep-sensor distance decreases the localization accuracy. To evaluate this effect, we fix the location of the footstep and increase the number of sensors. We employ two approaches for sensor selection: first, to mitigate the effect of distance, we randomly choose the subset of sensors; and second, to choose the optimal set of sensors using our approach, we choose the additional sensors based on the same principle (i.e., minimum distance to the footstep), as described in Section 4.4.1.

Fig. 11a shows the localization errors using the randomized sensor selection. The localization error decreases when the number of sensors increases up to six sensors, and then the error increases afterwards. Specifically, using four sensors results in 0.99 m average localization error; whereas, using six sensors and eight sensors results in 0.84 and 1.22 m average localization error. When we have a lower number of sensors, having sensors far from the footstep affects the localization results significantly. Due to randomized sensor selection, this is likely to happen and therefore utilizing four sensors results in the higher localization error than using six. On the other hand, if we have many sensors (e.g., eight) some of the sensors will be far from the footstep (regardless of the selection) and this results in large errors. Therefore, using the randomized sensor selection, six sensors result in minimum localization error.

Fig. 11b shows the localization errors using our sensor selection approach. In this case, by increasing the number of sensors, average localization error generally increases. Specifically, average localization error increases from 0.30 m using 4 sensors to 1.02 m using 8 sensors. The reason lies in our sensor selection algorithm which finds the closest sensors to the footstep location. In the four-sensor case, we choose the closest sensors to the footstep, which results in low localization error. Additional sensors will be further from the footstep and generally increase the localization error. Another observation in this figure is that the standard deviation of localization is decreased when we are using eight sensors instead of seven sensors. A similar trend is observed for cases with five and six sensors. This is because, in our experiments, the distance of the i^{th} and the $(i+1)^{th}$ furthest sensors from the footstep where i = 5, 7 are similar to each other, while for for i = 4, 6 the distances are significantly different (e.g., the 7^{th} and the 8^{th} furthest sensors are around the equal distance from the foot-

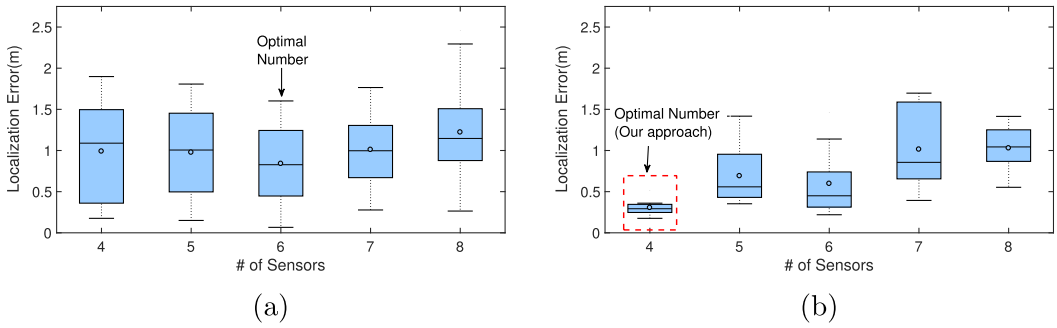

Fig. 11. Effect of number of sensors on localization accuracy. Part (a) is the localization results for randomized sensor selection and Part (b) shows the localization results using our sensor selection approach. The difference in the optimal number of sensors is because our approach chooses the closest sensors and therefore, the additional sensors will be further from the footstep and increase the localization error.

step while 6^{th} and the 7^{th} furthest sensors have different distances from the footstep). Therefore, adding the 7^{th} sensor further away from the other 6 sensors increased the estimation uncertainty compared to using 6 closest sensors, while adding the 8^{th} sensor decreased the estimation uncertainty since it adds more sensors without increasing the sensor distance from the 7^{th} sensor.

5.2.4. Robustness to Signal-to-Noise-Ratio (SNR)

To evaluate how our approach performs for different levels of noise, we investigate the relationship between localization performance and SNR relation. For each footstep event, SNR values are found by finding the ratio of the summed squared magnitude of the footstep-induced vibration signal to that of the noise (of the same length) and is described in decibel (db). The noise consists of ambient vibration measurements which does not include impulsive excitation and footstep events.To evaluate SNR and to separate the effect of SNR from the effect of distance, we use four sensors and localize footsteps at the same location. The overall SNR value for the system is computed as the average SNR of all the sensors. To consider the effect of different ranges of SNR, we have utilized two sensor configurations with two levels of sensing density.

The dense configuration consists of S4, S5, S7, and S8 and the sparse configuration consists of S1, S2, S7, and S8 as shown in Fig. 7. For the dense case, the Fig. 12a depicts the sensitivity of localization error with respect to the average SNR values. For this range of SNR values, the low correlation coefficient of 0.05 shows that localization error does not change significantly for different SNR values. The reason is that the energy (and resolution) of the footstep signals that are received is enough for accurate localization.

The sparser configuration consists of S1, S2, S7, and S8 (as shown in Fig. 7). The analysis for this case is presented in Fig. 12b. As discussed in Section 5.2.2, the sparse configuration generally shows larger localization errors due to the larger footstep-sensor distance. Furthermore, the effect of SNR values on the localization error is more significant (with correlation coefficient of -0.19). The reason lies in the fact that, due to higher distance, the footsteps can have lower energy and SNR values (lower than 12 db) for which the localization errors are large. However, low values of correlation coefficients for both cases show that our approach is robust to the noise level with SNR values above 12 db.

5.3. Dispersion mitigation evaluation

By focusing on the same set of frequency components in all the sensors, the wavelet-based signal decomposition approach mitigates the dispersion-related distortions and improves the localization accuracy. Fig. 13, Tables 2 and 3 compare the localization accuracy for the decomposed and raw signals. We estimate the location error using the Euclidean distance between the actual location and the estimated location of footsteps. In this figure, 'Raw' shows the results for the original signal; 'DecEn' shows the results for the extracted signals using the highest energy scales; 'DecSNR' shows the results for the extracted signals using the highest SNR scales; and finally, 'DecCost' shows the results for the extracted signals using the scale which result in the minimum localization cost. Specifically,this figure shows that, regardless of the multilateration solution approach (our adaptive approach or conventional nonlinear least square (NLS)) or the decomposition approach (highest energy scale (DecEn), highest SNR scale (DecSNR), or minimum localization cost scale (DecCost)), decomposing the signal improves the localization accuracy. Specifically, it decreases the localization error median between 1.41X and 2.48X (i.e., 41–148 percent)[1] and between 1.44X and 2.44X (i.e., 44–144 percent) using NLS and our solution approach, respectively.

[1] As an example, the percentage value in this case is found by calculating $(1.14 - 0.46)/0.46$ which corresponds to the percentage of increase in localization error for the baseline compared to our approach.

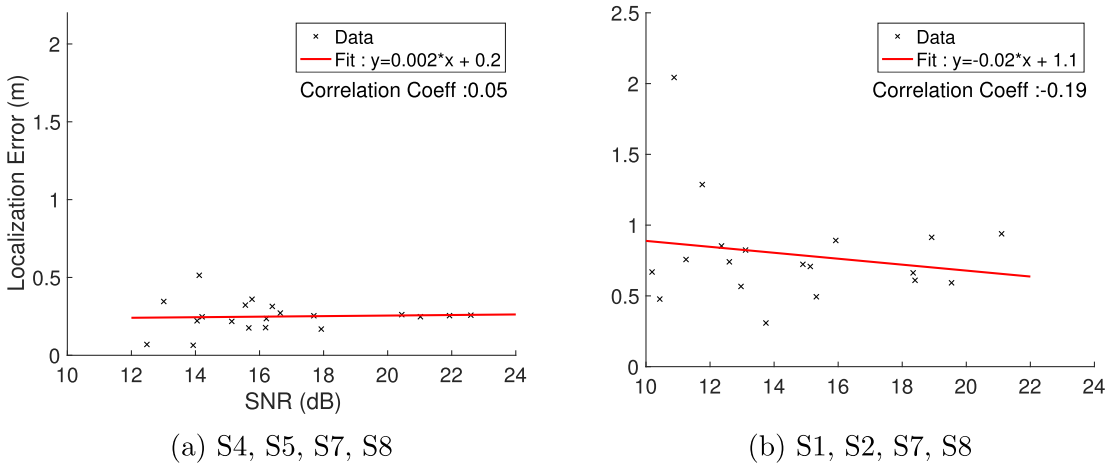

(a) S4, S5, S7, S8 (b) S1, S2, S7, S8

Fig. 12. Effect of SNR on localization accuracy. Parts (a) and (b) show the results for the denser and sparser sensor configurations, respectively. Because in the dense configuration the footsteps are generally received with high energy, the effects of SNR is negligible. However, in the sparse configuration, lower SNRs are possible and the decreasing trend of localization error with SNR is more significant.

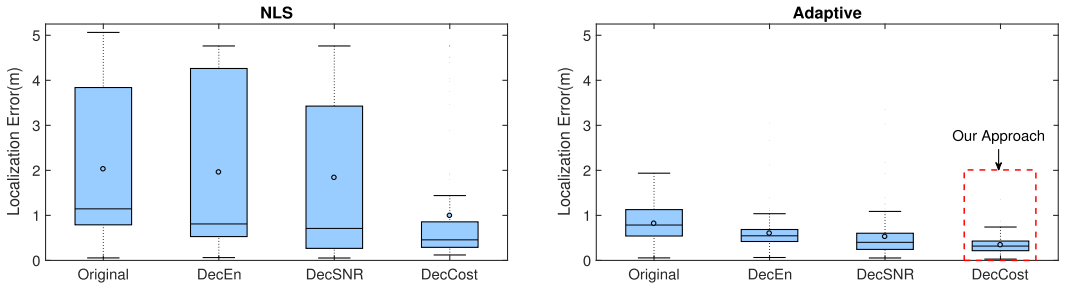

(a) (b)

Fig. 13. Localization accuracy evaluation: This figure shows the localization accuracy improvement achieved through signal decomposition. Part (a) displays the results using NLS and Part (b) displays the results using our adaptive solution approach. As can be seen, regardless of the localization and decomposition(i.e., component extraction) approach, signal decomposition improves the accuracy of localization.

Table 2
Localization improvement due to different signal decomposition methods (using NLS localization approach).

	Original	DecEn		DecSNR		DecCost (ours)	
	Error	Error	Improv.	Error	Improv.	Error	Improv.
Mean	2.03	1.96	1.04X	1.84	1.10X	0.99	2.05X
St. Dev.	1.57	1.78	0.88X	1.81	0.87X	1.33	1.18X
Median	1.14	0.81	1.41X	0.71	1.61X	0.46	2.48X
Quartile	3.04	3.73	0.82X	3.16	0.96X	0.57	5.33X

Table 3
Localization improvement due to different signal decomposition methods (using our adaptive multilateration approach).

	Original	DecEn		DecSNR		DecCost (Ours)	
	Error	Error	Improv.	Error	Improv.	Error	Improv.
Mean	0.82	0.6	1.37X	0.53	1.55X	0.34	2.41X
St. Dev.	0.4	0.4	1.00X	0.48	0.83X	0.18	2.22X
Median	0.79	0.55	1.44X	0.4	1.98X	0.32	2.47X
Quartile	0.59	0.27	2.19X	0.36	1.64X	0.21	2.81X

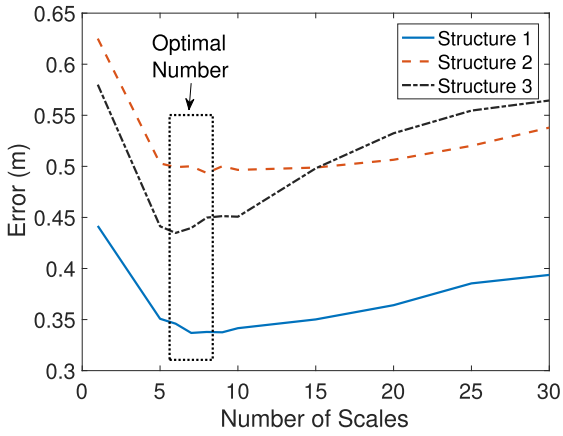

Fig. 14. Sensitivity to the number of scales: This figure shows the changes in the localization performance for different number of utilized scale components. The localization error is minimum for cases with 6–8 components and is fairly similar for cases with 5–10 components used in all the structures. Therefore, we use eight scale components for final estimation of footstep location.

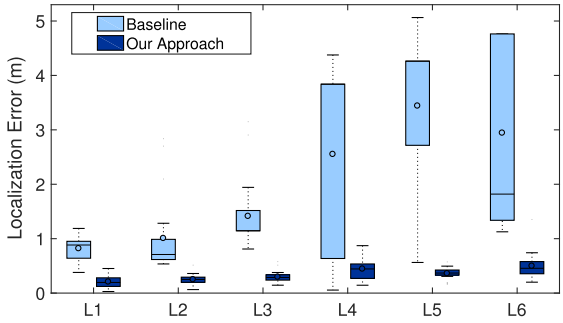

Fig. 15. Localization errors for different locations.

An important factor that needs to be decided is the number of scales which are used for occupant localization. The trade-off here is that: (1) using the average of estimated locations for several scale components reduces the effect of noisy estimations and outliers and improves localization performance; however, (2) including scale components that contain large level of noise will result in large localization error (even after averaging). Fig. 14 presents this trade-off and shows how the localization accuracy changes with the number of scale components for three structures. It can be seen that, for all three structures, the localization error is relatively similar for 5–10 scales. Therefore, choosing any of these numbers does not change the localization accuracy significantly. In this work, we empirically choose 8 scale components to estimate the footstep location through finding the average of estimated locations.

5.4. Locally adaptive localization evaluation

We evaluate performance improvements resulting from the use of our multilateration solution approach through the following steps: (1) evaluating robustness in different locations in one structure (to validate the robustness in heterogeneous floors), (2) evaluating robustness in various structures without calibration, and (3) comparing with a calibration-based method which assumes the wave propagation velocity.

5.4.1. Robustness to floor heterogeneity

To validate the robustness of our approach in heterogeneous floors, we compare the performance of our approach with a baseline approach for footsteps in six locations (as shown in Fig. 7). The baseline approach utilizes the raw signals for TDoA estimation and NLS multilateration solution, as mentioned in Section 5.2.1. This comparison is presented in Fig. 15 and Tables 4 and 5. These results show that our approach outperforms the baseline approach in all the locations. The average localization accuracy using our approach is 0.21–0.5 m. Compared to the baseline approach, these averages correspond to 3.9X–9.6X improvement. Similarly, our approach reduces the standard deviation (corresponding to the localization precision) by 1.9X–14.3X in different locations. Low localization error and consistent improvement in all the locations show that our approach performs well in real-world heterogeneous floors.

Table 4
Localization accuracy for locations 1, 2, and 3 (shown in Fig. 7).

	L1			L2			L3		
	Base	Ours	Imp.	Base	Ours	Imp.	Base	Ours	Imp.
Mean	0.82	0.21	3.9X	1.00	0.25	4.0X	1.41	0.29	4.9X
St. Dev.	0.21	0.11	1.9X	0.70	0.10	7.0X	0.63	0.11	5.7X
Median	0.88	0.20	4.4X	0.71	0.25	2.8X	1.14	0.29	3.9X
Quart.	0.31	0.16	1.9X	0.37	0.09	4.1X	0.37	0.10	3.7X

Table 5
Localization accuracy for locations 4, 5, and 6 (shown in Fig. 7).

	L4			L5			L6		
	Base	Ours	Imp.	Base	Ours	Imp.	Base	Ours	Imp.
Mean	2.55	0.44	5.8X	3.44	0.36	9.6X	2.94	0.50	5.9X
St. Dev.	1.70	0.2	8.5X	1.57	0.11	14.3X	1.68	0.25	6.7X
Median	3.84	0.44	8.7X	4.26	0.37	11.5X	1.82	0.46	4.0X
Quart.	3.2	0.27	11.9X	1.55	0.09	17.2X	3.42	0.22	15.5X

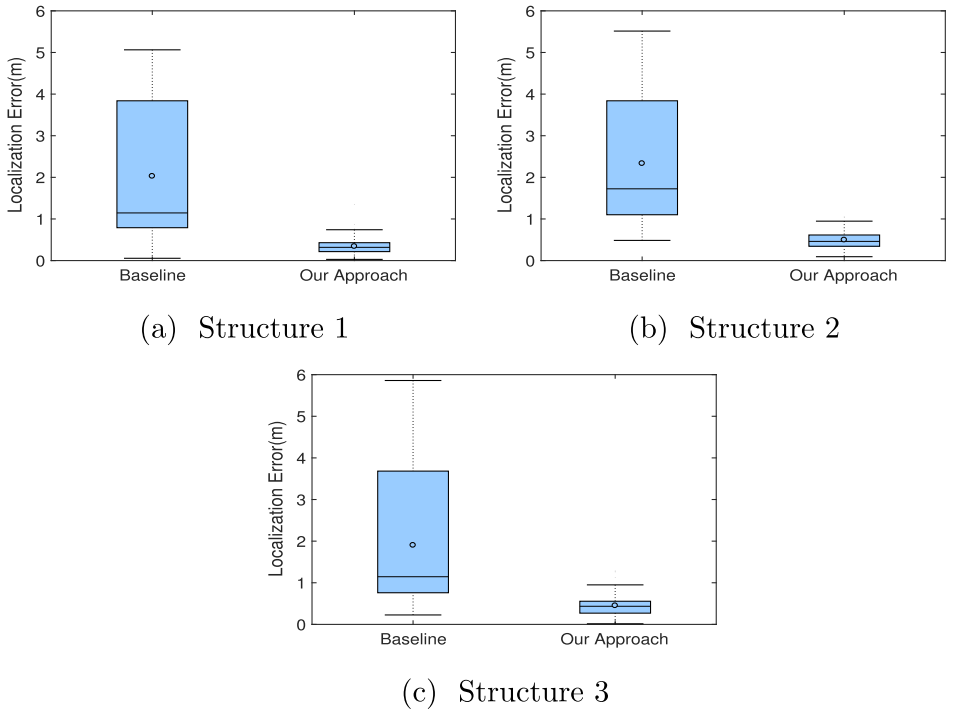

Fig. 16. Evaluating our localization approach in different structures. Part (a), Part (b), and Part (c) evaluates our approach in a non-carpeted wooden floor, a carpeted metal deck floor, and a non-carpeted concrete floor on ground level, respectively. Consistent improvement of localization performance in all the structures suggests that our locally adaptive localization approach is robust in different structures.

5.4.2. Robustness in different structures

To evaluate the robustness of our approach in different structures, we localized occupants in three structures, as described in Section 5.1. Fig. 16 and Table 6 compares the localization accuracy using our approach with that of a baseline approach in each structure. The first structure is a non-carpeted wooden floor on the second level of a residential building in Pittsburgh, PA. For this case, our approach resulted in 5.97X (i.e., 497 percent) improvement in the average localization accuracy, as well as 7.24X (i.e., 624 percent) improvement in localization precision. The second structure we evaluated is a carpeted concrete metal deck floor on the second level of a senior care facility in Pittsburgh, PA. For this structure, our approach improves the average localization accuracy and precision by an order of 4.66X (i.e., 366 percent) and 7.24X (i.e., 624 percent). The last structure we evaluated is a non-carpeted concrete floor on the ground level of a university campus building in

Table 6
Localization results for the three structures.

	Structure 1			Structure 2			Structure 3		
	Base	Ours	Imp.	Base	Ours	Imp.	Base	Ours	Imp.
Mean	2.03	0.34	5.97X	2.33	0.5	4.66X	1.90	0.45	4.22X
St. Dev.	1.57	0.18	8.72X	1.52	0.21	7.24X	1.52	0.25	6.08X
Median	1.15	0.32	3.59X	1.72	0.46	3.74X	1.15	0.43	2.67X
Quart.	3.05	0.21	14.52X	2.74	0.27	10.15X	2.92	0.29	10.07X

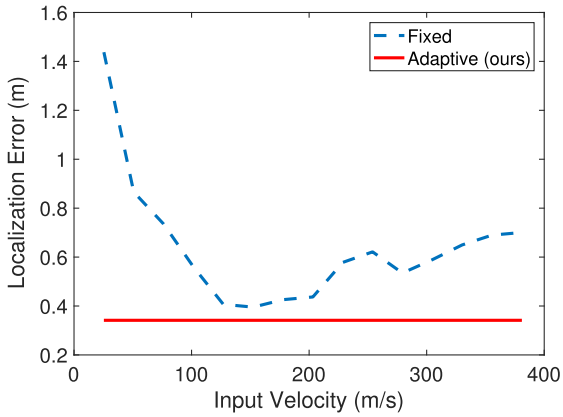

Fig. 17. Comparing the adaptive and the fixed-velocity localization approaches. This figure shows that, regardless of the assumed propagation velocity, our adaptive localization approach outperforms the fixed-velocity approach.

Pittsburgh, PA. In this structure, our approach results in 4.22X (i.e., 322 percent) and 6.08X (i.e., 508 percent) improvement in localization accuracy and precision.

In summary, We improve the localization accuracy between 4.22 and 5.97 times the baseline approach in different structures and also improve the localization precision between 6.08 and 8.72 times. The consistent improvement in a range of structures further shows that our approach is robust to structural differences.

5.5. Calibration evaluation

In this section, we compare our locally adaptive approach with a calibration-based approach which assumes a fixed wave propagation velocity in the floor and obtains its value through a calibration before the run-time occupant localization (fixed-velocity approach) [26]. Fig. 17 shows the average localization accuracy of the fixed-velocity approach for different wave propagation velocity calibrations and compares it to our adaptive approach. Our approach does not require the wave propagation velocity as an input and hence its localization errors does not change for varying velocity inputs (and hence it is represented by the flat line). However, the performance of the fixed-velocity approach depends on the assumed velocity input. This figure shows that the fixed-velocity approach results in the minimum localization error of 0.39 m when the calibrated wave propagation velocity is equal to 152.4 m/s. On the other hand, our approach (with adaptive velocity) results in 0.34 m of localization error and, as it does not depend on the velocity, it is shown with a constant line. Therefore, our approach outperforms the fixed case regardless of the assumed wave propagation velocity. The reason is that the assumption of a fixed velocity for all the footstep locations does not hold in real-world floors which contain spatial structural variations. Our approach does not make such an assumption and thus can better deal with these structural variations.

6. Discussion and future work

- Our unoptimized localization algorithm is implemented in Matlab 2016b. The computation time of the current implementation is 1.6 s for each footstep on a server pc (Intel Core i7-7820X processor with 8 cores). This computation time can be further reduced through: (1) code-optimization using more optimized languages; and (2) lower sampling frequency (or undersampling) considering the wave propagation velocity range of the lamb wave.
- In this paper, our assumption is that the wave propagation is not obstructed by structural and non-structural elements (e.g., walls, beams). In most residential and commercial buildings, this assumption is valid for within each room and sections of hallways. The reason is that each room or a section of hallway is part of the structural bay, and therefore there is no obstruction in the middle. Having obstructions might change the structural mass and stiffness and hence the wave

propagation properties (such as propagation velocity). This in turn may result in inaccurate localization. We have focused on this problem in our preliminary work [84] by assuming that the propagation velocity can potentially vary in different directions. As part of our future work, we plan to further extend this algorithm and make it robust to different types of obstructions in the structure.

- As discussed in Section 5.2.2, the localization approach performs well when the footsteps are inside the polygon formed by the sensors. However, the performance drops when footsteps outside the polygon are considered. As part of our future work, we plan to update the algorithm to improve its performance under this situation.
- This paper is focused on localizing footsteps caused by one person in each sensing area. In our preliminary work for multiple people localization, we have utilized the observation that, most of the time, people do not usually walk synchronously at the exact same time. Based on this observation, we have used the first peaks of the signals to detect the onsight of the footstep and estimate the TDoAs to localize multiple people [85]. To further improve the accuracy and robustness of this multiple people localization approach, we plan to incorporate tracking (sequence of locations in time).
- Finally, we will explore the applications of location information in smart buildings (e.g., energy management and space utilization).

7. Conclusions

In this paper, we introduce a robust and fine-grained occupant localization approach based on the footstep-induced floor vibrations for dispersive and heterogeneous floors. Our approach is non-intrusive to occupants and enables sparse sensor deployment compared to conventional methods such as pressure- and RF-based sensing. The main challenges are signal distortions due to dispersion and wave propagation velocity variation in different floor locations due to heterogeneity. We address dispersion-related signal distortions by decomposing the signal (using wavelet transform) and extracting specific components with similar propagation characteristics. We have chosen the components which result in highest localization performance. Moreover, we address the velocity variation by introducing an adaptive multilateration solution which does not require prior knowledge of the wave propagation velocity in the floor. Our evaluations show that: (1) regardless of the multilateration and decomposition (i.e., component extraction) approach, signal decomposition improves the accuracy of localization (e.g., 2.41X improvement in localization using our decomposition method compared to using the raw signal); (2) our locally adaptive localization approach for heterogeneous floors outperforms the baseline approach in different locations of the same structure with average errors of 0.21–0.5, which shows up to 9.6X improvement; (3) our approach performs well across different structures (with errors as low as 0.34 m location estimation error, which corresponds to 6X reduction compared to the baseline approach); (4) our approach does not assume a constant propagation velocity (i.e., adaptive) and therefore outperforms the calibration-based approach which assumes a fixed velocity. Our system provides an accurate and non-invasive sensing approach for indoor occupant localization and can significantly improve future smart building applications.

Acknowledgments

This research was partially supported by NSF (CNS-1149611 and CMMI-1653550), Google, Intel, Pennsylvania Infrastructure Technology Alliance, and CMU-SYSU Collaborative Innovation Research Center. The authors would also like to acknowledge Vincentian Nursing Home for providing deployment sites to conduct experiments and collect data.

References

[1] G. Diraco, A. Leone, P. Siciliano, People occupancy detection and profiling with 3d depth sensors for building energy management, Energy Build. 92 (2015) 246–266.
[2] C.M. Stoppel, F. Leite, Integrating probabilistic methods for describing occupant presence with building energy simulation models, Energy Build. 68 (2014) 99–107.
[3] A.J. Newman, K. Daniel, D.P. Oulton, New insights into retail space and format planning from customer-tracking data, J. Retail. Consum. Serv. 9 (5) (2002) 253–258.
[4] V. Uotila, P. Skogster, Space management in a diy store analysing consumer shopping paths with data-tracking devices, Facilities 25 (9/10) (2007) 363–374.
[5] D.R. Riley, V.E. Sanvido, Space planning method for multistory building construction, J. Constr. Eng. Manage. 123 (2) (1997) 171–180.
[6] .WP. Cully, S.L. Cotton, W.G. Scanlon, J. McQuiston, Localization algorithm performance in ultra low power active rfid based patient tracking, in: Personal Indoor and Mobile Radio Communications (PIMRC), 2011 IEEE 22nd International Symposium on, IEEE, 2011, pp. 2158–2162.
[7] W.P. Cully, S.L. Cotton, W.G. Scanlon, Empirical performance of rssi-based monte carlo localisation for active rfid patient tracking systems, Int. J. Wireless Inf. Networks 19 (3) (2012) 173–184.
[8] P. Henry, M. Krainin, E. Herbst, X. Ren, D. Fox, Rgb-d mapping: using kinect-style depth cameras for dense 3d modeling of indoor environments, Int. J. Robot. Res. 31 (5) (2012) 647–663.
[9] Y. Zhang, C. Luo, J. Liu, Walk&sketch: create floor plans with an rgb-d camera, in: Proceedings of the 2012 ACM Conference on Ubiquitous Computing, ACM, 2012, pp. 461–470.
[10] D. Savio, T. Ludwig, Smart carpet: a footstep tracking interface, in: Advanced Information Networking and Applications Workshops, 2007, AINAW'07. 21st International Conference on, Vol. 2, IEEE, 2007, pp. 754–760.
[11] M. Andries, O. Simonin, F. Charpillet, Localization of humans, objects, and robots interacting on load-sensing floors, IEEE Sens. J. 16 (4) (2016) 1026–1037.
[12] C. Xu, B. Firner, R.S. Moore, Y. Zhang, W. Trappe, R. Howard, F. Zhang, N. An, Scpl: Indoor device-free multi-subject counting and localization using radio signal strength, in: Proceedings of the 12th international conference on Information Processing in Sensor Networks, ACM, 2013, pp. 79–90.

[13] A.S. Paul, E.A. Wan, F. Adenwala, E. Schafermeyer, N. Preiser, J. Kaye, P.G. Jacobs, Mobilerf: a robust device-free tracking system based on a hybrid neural network hmm classifier, in: Proceedings of the 2014 ACM International Joint Conference on Pervasive and Ubiquitous Computing, ACM, 2014, pp. 159–170.
[14] J.T. Biehl, M. Cooper, G. Filby, S. Kratz, Loco: a ready-to-deploy framework for efficient room localization using wi-fi, in: Proceedings of the 2014 ACM International Joint Conference on Pervasive and Ubiquitous Computing, ACM, 2014, pp. 183–187.
[15] A. Purohit, Z. Sun, S. Pan, P. Zhang, Sugartrail: Indoor navigation in retail environments without surveys and maps, in: Sensor, Mesh and Ad Hoc Communications and Networks (SECON), 2013 10th Annual IEEE Communications Society Conference on, IEEE, 2013, pp. 300–308.
[16] P. Lazik, N. Rajagopal, O. Shih, B. Sinopoli, A. Rowe, Alps: A bluetooth and ultrasound platform for mapping and localization, in: Proceedings of the 13th ACM Conference on Embedded Networked Sensor Systems, ACM, 2015, pp. 73–84.
[17] E. Martin, O. Vinyals, G. Friedland, R. Bajcsy, Precise indoor localization using smart phones, in: Proceedings of the international conference on Multimedia, ACM, 2010, pp. 787–790.
[18] A. Rai, K.K. Chintalapudi, V.N. Padmanabhan, R. Sen, Zee: zero-effort crowdsourcing for indoor localization, in: Proceedings of the 18th annual international conference on Mobile computing and networking, ACM, 2012, pp. 293–304.
[19] K. Chintalapudi, A. Padmanabha Iyer, V.N. Padmanabhan, Indoor localization without the pain, in: Proceedings of the sixteenth annual international conference on Mobile computing and networking, ACM, 2010, pp. 173–184.
[20] V. Lenders, E. Koukoumidis, P. Zhang, M. Martonosi, Location-based trust for mobile user-generated content: applications, challenges and implementations, in: Proceedings of the 9th workshop on Mobile computing systems and applications, ACM, 2008, pp. 60–64.
[21] R. Bahroun, O. Michel, F. Frassati, M. Carmona, J. Lacoume, New algorithm for footstep localization using seismic sensors in an indoor environment, J. Sound Vib. 333 (3) (2014) 1046–1066.
[22] A.G. Woolard, V.S. Malladi, P.A. Tarazaga, et al., Classification of event location using matched filters via on-floor accelerometers, in: SPIE Smart Structures and Materials+ Nondestructive Evaluation and Health Monitoring, International Society for Optics and Photonics, 2017, pp. 101681A–101681A.
[23] J.D. Poston, R.M. Buehrer, P.A. Tarazaga, Indoor footstep localization from structural dynamics instrumentation, Mech. Syst. Signal Process. 88 (2017) 224–239.
[24] M. Mirshekari, P. Zhang, H.Y. Noh, Non-intrusive occupant localization using floor vibrations in dispersive structure, in: Proceedings of the 14th ACM Conference on Embedded Network Sensor Systems CD-ROM, ACM, 2016, pp. 378–379.
[25] S. Pan, T. Yu, M. Mirshekari, J. Fagert, A. Bonde, O.J. Mengshoel, H.Y. Noh, P. Zhang, Footprintid: Indoor pedestrian identification through ambient structural vibration sensing, IMWUT 1 (2017) 89:1–89:31.
[26] M. Mirshekari, S. Pan, P. Zhang, H.Y. Noh, Characterizing wave propagation to improve indoor step-level person localization using floor vibration, in: SPIE Smart Structures and Materials+ Nondestructive Evaluation and Health Monitoring, International Society for Optics and Photonics, 2016, pp. 980305–980305.
[27] J.S. Hall, J.E. Michaels, Model-based parameter estimation for characterizing wave propagation in a homogeneous medium, Inverse Prob. 27 (3) (2011) 035002.
[28] A. Raghavan, C.E. Cesnik, Guided-wave signal processing using chirplet matching pursuits and mode correlation for structural health monitoring, Smart Mater. Struct. 16 (2) (2007) 355.
[29] J. Jiao, C. He, B. Wu, R. Fei, X. Wang, Application of wavelet transform on modal acoustic emission source location in thin plates with one sensor, Int. J. Press. Vessels Pip. 81 (5) (2004) 427–431.
[30] N. Toyama, J.-H. Koo, R. Oishi, M. Enoki, T. Kishi, Two-dimensional ae source location with two sensors in thin cfrp plates, J. Mater. Sci. Lett. 20 (19) (2001) 1823–1825.
[31] W. Prosser, M.D. Seale, B.T. Smith, Time-frequency analysis of the dispersion of lamb modes, J. Acoust. Soc. Am. 105 (5) (1999) 2669–2676.
[32] F. Ciampa, M. Meo, Acoustic emission source localization and velocity determination of the fundamental mode a0 using wavelet analysis and a newton-based optimization technique, Smart Mater. Struct. 19 (4) (2010) 045027.
[33] H. Jeong, Y.-S. Jang, Wavelet analysis of plate wave propagation in composite laminates, Compos. Struct. 49 (4) (2000) 443–450.
[34] H. Jeong, Y.-S. Jang, Fracture source location in thin plates using the wavelet transform of dispersive waves, Ultrason. Ferroelectrics Frequency Control IEEE Trans. 47 (3) (2000) 612–619.
[35] F. Li, G. Meng, L. Ye, Y. Lu, K. Kageyama, Dispersion analysis of lamb waves and damage detection for aluminum structures using ridge in the time-scale domain, Meas. Sci. Technol. 20 (9) (2009) 095704.
[36] A. Perelli, L. De Marchi, A. Marzani, N. Speciale, Frequency warped cross-wavelet multiresolution analysis of guided waves for impact localization, Signal Process. 96 (2014) 51–62.
[37] E.D. Niri, S. Salamone, A probabilistic framework for acoustic emission source localization in plate-like structures, Smart Mater. Struct. 21 (3) (2012) 035009.
[38] S. Coraluppi, Multistatic sonar localization, IEEE J. Oceanic Eng. 31 (4) (2006) 964–974.
[39] E. Hoppe, M. Roan, Non-linear, adaptive array processing for underwater source localization and sonar interference suppression, in: OCEANS 2009-EUROPE, IEEE, 2009, pp. 1–5.
[40] J.J. Caffery Jr., Wireless location in CDMA cellular radio systems, Vol. 53, Springer Science & Business Media, 2006.
[41] S.T. Chia, Location determination and handover in mobile radio systems, uS Patent 5,394,158 (February 28, 1995).
[42] X. Sheng, Y.-H. Hu, Maximum likelihood multiple-source localization using acoustic energy measurements with wireless sensor networks, IEEE Trans. Signal Process. 53 (1) (2005) 44–53.
[43] M.G. Rabbat, R.D. Nowak, Decentralized source localization and tracking [wireless sensor networks], in: Acoustics, Speech, and Signal Processing, 2004. Proceedings.(ICASSP'04). IEEE International Conference on, Vol. 3, IEEE, 2004, pp. iii–921.
[44] F. Ciampa, M. Meo, A new algorithm for acoustic emission localization and flexural group velocity determination in anisotropic structures, Compos. A: Appl. Sci. Manuf. 41 (12) (2010) 1777–1786.
[45] A. Perelli, L. De Marchi, A. Marzani, N. Speciale, Acoustic emission localization in plates with dispersion and reverberations using sparse pzt sensors in passive mode, Smart Mater. Struct. 21 (2) (2012) 025010.
[46] T. Kundu, Acoustic source localization, Ultrasonics 54 (1) (2014) 25–38.
[47] J.-M. Valin, F. Michaud, J. Rouat, D. Létourneau, Robust sound source localization using a microphone array on a mobile robot, in: Intelligent Robots and Systems, 2003.(IROS 2003). Proceedings. 2003 IEEE/RSJ International Conference on, Vol. 2, IEEE, 2003, pp. 1228–1233.
[48] K. Nakadai, D. Matsuura, H.G. Okuno, H. Kitano, Applying scattering theory to robot audition system: robust sound source localization and extraction, in: Intelligent Robots and Systems, 2003.(IROS 2003). Proceedings. 2003 IEEE/RSJ International Conference on, Vol. 2, IEEE, 2003, pp. 1147–1152.
[49] T. He, Q. Pan, Y. Liu, X. Liu, D. Hu, Near-field beamforming analysis for acoustic emission source localization, Ultrasonics 52 (5) (2012) 587–592.
[50] J.C. Chen, K. Yao, R.E. Hudson, Source localization and beamforming, IEEE Signal Process. Mag. 19 (2) (2002) 30–39.
[51] J.-M. Valin, F. Michaud, J. Rouat, Robust localization and tracking of simultaneous moving sound sources using beamforming and particle filtering, Robot. Auton. Syst. 55 (3) (2007) 216–228.
[52] S.P. Tarzia, P.A. Dinda, R.P. Dick, G. Memik, Indoor localization without infrastructure using the acoustic background spectrum, in: Proceedings of the 9th international conference on Mobile systems, applications, and services, ACM, 2011, pp. 155–168.
[53] M. Azizyan, I. Constandache, R. Roy Choudhury, Surroundsense: mobile phone localization via ambience fingerprinting, in: Proceedings of the 15th annual international conference on Mobile computing and networking, ACM, 2009, pp. 261–272.
[54] E.C. Chan, G. Baciu, S. Mak, Using wi-fi signal strength to localize in wireless sensor networks, in: Communications and Mobile Computing, 2009. CMC'09. WRI International Conference on, Vol. 1, IEEE, 2009, pp. 538–542.

[55] Q. Fu, G. Retscher, Active rfid trilateration and location fingerprinting based on rssi for pedestrian navigation, J. Navigation 62 (02) (2009) 323–340.
[56] N.K. Sharma, A weighted center of mass based trilateration approach for locating wireless devices in indoor environment, in: Proceedings of the 4th ACM international workshop on Mobility management and wireless access, ACM, 2006, pp. 112–115.
[57] Y. Xu, J. Zhou, P. Zhang, Rss-based source localization when path-loss model parameters are unknown, Commun. Lett. IEEE 18 (6) (2014) 1055–1058.
[58] Y. Zhou, J. Li, L. Lamont, Multilateration localization in the presence of anchor location uncertainties, in: Global Communications Conference (GLOBECOM), 2012 IEEE, IEEE, 2012, pp. 309–314.
[59] D. Liang, S.-f. Yuan, M.-l. Liu, Distributed coordination algorithm for impact location of preciseness and real-time on composite structures, Measurement 46 (1) (2013) 527–536.
[60] T. Kundu, S. Das, S.A. Martin, K.V. Jata, Locating point of impact in anisotropic fiber reinforced composite plates, Ultrasonics 48 (3) (2008) 193–201.
[61] K.W. Cheung, H.-C. So, W.-K. Ma, Y.-T. Chan, Least squares algorithms for time-of-arrival-based mobile location, IEEE Trans. Signal Process. 52 (4) (2004) 1121–1130.
[62] F. Gustafsson, F. Gunnarsson, Positioning using time-difference of arrival measurements, in: Acoustics, Speech, and Signal Processing, 2003. Proceedings.(ICASSP'03). 2003 IEEE International Conference on, Vol. 6, IEEE, 2003, pp. VI–553.
[63] G. Destino, G. Abreu, On the maximum likelihood approach for source and network localization, IEEE Trans. Signal Process. 59 (10) (2011) 4954–4970.
[64] Y.-T. Chan, H.Y.C. Hang, P.-c. Ching, Exact and approximate maximum likelihood localization algorithms, IEEE Trans. Veh. Technol. 55 (1) (2006) 10–16.
[65] G. Yan, J. Tang, A bayesian approach for localization of acoustic emission source in plate-like structures, Math. Probl. Eng. (2015).
[66] I.A. Viktorov, Rayleigh and Lamb Waves: Physical Theory and Applications, Plenum Press, 1970.
[67] Y.H. Lee, T. Oh, The simple lamb wave analysis to characterize concrete wide beams by the practical masw test, Materials 9 (6) (2016) 437.
[68] K. Worden, Rayleigh and lamb waves-basic principles, Strain 37 (4) (2001) 167–172.
[69] Y.H. Lee, T. Oh, The measurement of p-, s-, and r-wave velocities to evaluate the condition of reinforced and prestressed concrete slabs, Adv. Mater. Sci. Eng. (2016).
[70] S. Pan, S.P. Xu, M. Mirshekari, P. Zhang, H.Y. Noh, Collaboratively adaptive vibration sensing system for high fidelity monitoring of structural responses induced by pedestrians, Front. Built Environ. 3 (2017) 28.
[71] M. Lam, M. Mirshekari, S. Pan, P. Zhang, H.Y. Noh, Robust occupant detection through step-induced floor vibration by incorporating structural characteristics, Dyn. Coupled Struct., Vol. 4, Springer, 2016, pp. 357–367.
[72] M. Mirshekari, P. Zhang, H.Y. Noh, Calibration-free footstep frequency estimation using structural vibration, Dyn. Civil Struct., Vol. 2, Springer, 2017, pp. 287–289.
[73] M. Baron, Probability and Statistics for Computer Scientists, CRC Press, 2013.
[74] T. Finch, Incremental Calculation of Weighted Mean and Variance, University of Cambridge 4 (2009) 11–15.
[75] P.S. Addison, The illustrated wavelet transform handbook: introductory theory and applications in science, engineering, medicine and finance, CRC Press, 2002.
[76] M. Edwards, X. Xie, Footstep pressure signal analysis for human identification, in: Biomedical Engineering and Informatics (BMEI), 2014 7th International Conference on, IEEE, 2014, pp. 307–312.
[77] J.M. Sabatier, A.E. Ekimov, A review of human signatures in urban environments using seismic and acoustic methods, in: Technologies for Homeland Security, 2008 IEEE Conference on, IEEE, 2008, pp. 215–220.
[78] M. Alaziz, Z. Jia, J. Liu, R. Howard, Y. Chen, Y. Zhang, Motion scale: a body motion monitoring system using bed-mounted wireless load cells, in: Connected Health: Applications, Systems and Engineering Technologies (CHASE), 2016 IEEE First International Conference on, IEEE, 2016, pp. 183–192.
[79] I/O Sensor Nederland bv, SM-24 Geophone Element, p/N 1004117 (2006).
[80] S. Pan, M. Mirshekari, J. Fagert, C.G. Ramirez, A.J. Chung, C.C. Hu, J.P. Shen, P. Zhang, H.Y. Noh, Characterizing human activity induced impulse and slip-pulse excitations through structural vibration, J. Sound Vib. 414 (2018) 61–80.
[81] J.A. Paradiso, C. King Leo, Tracking and characterizing knocks atop large interactive displays, Sens. Rev. 25 (2) (2005) 134–143.
[82] M. Abramowitz, I.A. Stegun, Handbook of mathematical functions: with formulas, graphs, and mathematical tables, Vol. 55, Courier Corporation, 1964.
[83] D. Schwarz, Fast and robust curve intersections, http://www.mathworks.com/matlabcentral/fileexchange/11837-fast-and-robust-curve-intersections, [Online; accessed 13-September-2016] (2010).
[84] M. Mirshekari, J. Fagert, S. Pan, P. Zhang, H. Noh, Occupant localization in obstructed indoor environments using floor vibrations, in: Engineering Mechanics Institute Conference 2017, EMI, 2017.
[85] S. Pan, K. Lyons, M. Mirshekari, H.Y. Noh, P. Zhang, Multiple pedestrian tracking through ambient structural vibration sensing, in: SenSys, 2016, pp. 366–367.